

Green Chemistry

Accepted Manuscript



This is an *Accepted Manuscript*, which has been through the Royal Society of Chemistry peer review process and has been accepted for publication.

Accepted Manuscripts are published online shortly after acceptance, before technical editing, formatting and proof reading. Using this free service, authors can make their results available to the community, in citable form, before we publish the edited article. We will replace this *Accepted Manuscript* with the edited and formatted *Advance Article* as soon as it is available.

You can find more information about *Accepted Manuscripts* in the [Information for Authors](#).

Please note that technical editing may introduce minor changes to the text and/or graphics, which may alter content. The journal's standard [Terms & Conditions](#) and the [Ethical guidelines](#) still apply. In no event shall the Royal Society of Chemistry be held responsible for any errors or omissions in this *Accepted Manuscript* or any consequences arising from the use of any information it contains.



www.rsc.org/greenchem

ARTICLE

New bi-functional zinc catalysts based on robust and easy-to-handle *N*-chelating ligands for the synthesis of cyclic carbonates from epoxides and CO₂ under mild conditions

Rongchang Luo, Xiantai Zhou, Wuying Zhang, Zhongxiu Liang, Jun Jiang and Hongbing Ji*

A series novel zinc complexes were prepared by covalent linkage of various imidazolium-based ionic liquid moieties with the 2,2'-bipyridine ligand at the two sides of the 4,4'-position. The zinc(II) complexes containing the rigid *N*-chelating ligand proved to be stable, highly efficient and easy-to-handle catalysts towards the synthesis of cyclic carbonate from epoxide and CO₂ without the use of any co-catalysts or organic solvent. The catalysts can be easily recovered and reused without significant loss of activity and selectivity by control of solvent. The kinetic study uncovered that the reaction was first-order with respect to epoxide. Moreover, a plausible reaction mechanism was proposed, in which zinc center could promote ring-opening of the epoxide for the synergetic effect with the anion X⁻ within ILs.

Introduction

It is well-known that CO₂ is the major greenhouse gas suspected to cause global warming. In terms of the so-called “sustainable society” and “green chemistry” concepts, the effective utilization of carbon dioxide as a safe, cheap, abundant renewable and environmentally benign C1 building block in organic synthesis, has attracted much attention both from industrial and academic viewpoints.¹ In this regard, the synthesis of five-membered cyclic carbonates *via* the 100 % atom-economical coupling reactions of CO₂ and epoxides under mild condition is one of a few industrial synthetic processes in this area.² On the other hand, cyclic carbonates are widely used as electrolyte components for lithium batteries, polar aprotic solvents, and intermediates in the production of pharmaceuticals and fine chemicals.³

In the past few decades, numerous homogeneous catalytic systems such as metal oxides,⁴ quaternary onium salt,⁵ alkali metal halides,⁶ ionic liquids (ILs),⁷ transition metal complexes,⁸ *N*-heterocyclic carbenes (NHC),⁹ functional organic polymers¹⁰ have been developed for promoting these transformations, which usually could be operated under much milder conditions than heterogeneous catalytic systems. Amongst such processes, transition metal-based complexes in conjunction with Lewis base (such as onium salt) have been employed as the high-efficiency binary catalysts under relatively mild conditions (even room temperature and 1 atm pressure¹¹). Meanwhile, various quaternary ammonium or phosphonium groups were recently introduced into the frame of the nitrogen-containing ligands (*e.g.* N₂O₂-ligand: salen¹² or N₄-ligand: porphyrin¹³), thus leading to a series of novel bi-functional metal catalysts in one molecule. More interestingly, these single-component analogues could be easily recovered and reused by

adding organic solvent (*e.g.* ether or ester). Consequently, the efficient reusability of the catalyst makes the process more economically and potentially viable for commercial application.^{12a}

For the cycloaddition of CO₂ to epoxide, activation of epoxide and subsequent epoxide ring opening are vital steps.¹⁴ Fig. 1 shows a catalytic motif for the double activation of an epoxide with this type of catalyst. In general, the cooperative action of an anion X⁻ (nucleophilic) and a metal centre M (Lewis acid) promotes the ring-opening of epoxide.^{13a} Hence, it seems to be currently the most promising candidates with one particular trend as far as the catalyst design is concerned: the grafting of ionic moieties on the ligand backbone could perform as co-catalysts.¹⁵ Obviously, bi-functionality has proven to be highly useful in various cases to create more powerful catalyst mediators.^{12h} However, this category of catalyst have being less developed as a probable result of the more synthetically demanding characteristics of bi-functional catalyst preparation.

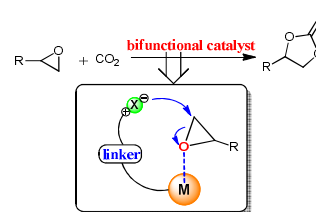


Fig. 1 Cooperative activation of epoxide with bi-functional catalyst

Based on the above strategies, our group ever developed various salen aluminum complexes functionalized by polyether-based imidazolium ILs, which were used as high efficient, bi-functional and homogeneous catalysts for the cycloaddition of CO₂ to epoxides under mild conditions (100 °C, 1.0 MPa) without the addition of co-catalyst or organic solvent. Meanwhile, the catalysts presented

excellent “CO₂ capture” capability due to the weak interaction between the CO₂ molecule and the PEO chain.¹⁶ However, using zinc instead of aluminum as a metal center, it was disappointed that the similar Zn-containing catalyst presented lower activity with low TOF value under the identical conditions.

2,2'-Bipyridine ligands are currently attracting a great deal of interest as the another nitrogen-containing ligand, which readily to interact with the metals *via* both σ -donating nitrogen atoms and π -accepting molecule orbitals.¹⁷ Metal complex containing the rigid chelating 2,2'-bipyridine ligand was regarded as efficient catalysts capable of carrying out various catalytic reactions under mild reaction conditions.¹⁸ Besides, the resulting complexes were very stable due to the formation of a five-membered chelate. However, to date, only few studies explored the type of metal complex in the formation of cyclic carbonates.¹⁹ Zinc as a kind of a strong Lewis acid and nontoxic metal, is a better choice for CO₂ coupling with epoxides.^{12h, 20} Therefore, 2,2'-bipyridine zinc(II) complexes can potentially facilitate for the cycloaddition reaction.

With this idea in mind, a new bi-functional 2,2'-bipyridine zinc(II) complexes bearing various IL moieties in one molecule were designed and synthesized. We initiated our study by examining the catalytic activity of the cycloaddition reaction of allyl glycidyl ether (AGE) with CO₂. It was found these Zn-containing catalysts were proved to be stable, efficient and easy-to-handle catalysts towards the synthesis of cyclic carbonate from epoxide and CO₂ under solvent-free condition in the absence of a co-catalyst. Meanwhile, we envisaged that the cooperative action between an anion X⁻ (nucleophile) within ILs and a metal center (Lewis acid). The large-scale synthesis of styrene cyclic carbonate (SC) catalyzed by 2,2'-bipyridine zinc(II) complexes was carried out and >90% yield could be obtained. Furthermore, the kinetics and mechanism of the reaction were investigated *via* the *in situ* IR spectroscopy.

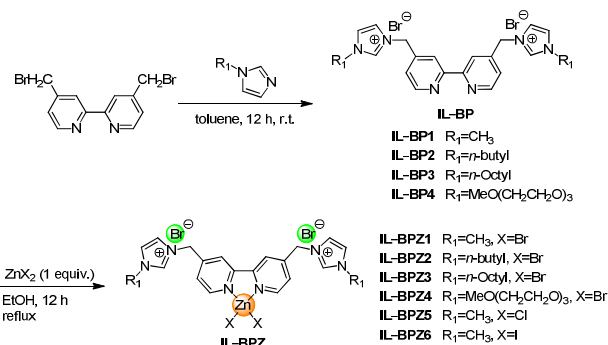
Results and Discussion

Synthesis of catalysts

Because the catalytic performances of these Zn-containing catalysts are affected by the anion and/or ligand bonding to the zinc ion center, we choose zinc salts containing halide ions (*e.g.* Cl⁻, Br⁻, I⁻) as metal coordinating center due that halide anions were used as simple coordinating ligands to form a tetrahedral environment around the zinc ion.²¹ It is worth noting that an acidic metal center could coordinate with the epoxide in the coupling reaction, whereas a *N*-chelating ligand with suitable geometry and a leaving group may easily form a reactive metal-alkoxide bond.¹⁵

The synthesis route for IL-functionalized 2,2'-bipyridine zinc(II) complexes (denoted as **IL-BPZ**) was shown in **Scheme 1**. In the first place, *N*-alkyl imidazole was added dropwise into the stirred suspension including 4,4'-dibromomethyl-2,2'-bipyridine²² in toluene (or acetone) solution at room temperature under nitrogen atmosphere. *N*-Alkyl-3-methyleneimidazolium bromide modified 2,2'-bipyridine ligand (denoted as **IL-BP**) was obtained immediately. Then, after metalation with ZnX₂ (X = Cl, Br, I) in ethanol, it resulted in the corresponding 2,2'-bipyridine zinc(II)

complex **IL-BPZ** as white powder (**Scheme 1**).²³ Additionally, complex **IL-BPZ7** was prepared by ion-exchange method in the NaBF₄ water solution. Following the similar procedure, **IL-BPZ8** was also obtained with a high yield using 4-methylpyridine instead of *N*-methylimidazole (**Chart 1**). It is particularly worth mentioning that these complexes were stable in air and soluble in water, DMF, ether and ester. For comparison, the simple 2,2'-bipyridine zinc(II) complex **BPZ** and the traditional ionic liquid (1-benzyl-3-methylimidazolium bromide, denoted as **IL**) were also prepared according the similar method in the literature (**Chart 1**).²¹



Scheme 1 Synthetic route for various IL-functionalized 2,2'-bipyridine zinc(II) complexes **IL-BPZ**.

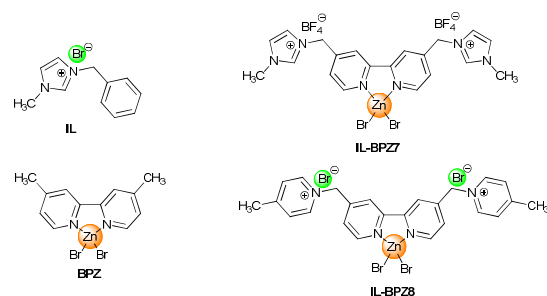


Chart 1 Structures of catalyst **IL**, **BPZ**, **IL-BPZ7** and **IL-BPZ8**.

Characterization of catalysts

Initially, the ¹H NMR of catalyst **IL-BPZ1** and the corresponding ligand **IL-BP1** were firstly recorded on Bruker AV 400M in DMSO-*d*₆ for the structure characterization. As show in **Fig. 2**, some peaks at 8.74-8.76, 8.40, 7.49-7.50 ppm originated from the proton of pyridine ring, and also at 9.41, 7.93, 7.83 ppm originated from the proton of imidazolium ring were observed in the ¹H NMR spectrum of **IL-BP1**. It is proposed that the new peak at 5.68 ppm due to methylene group resulted from the reaction between bromomethyl group (-CH₂Br) at the 4,4'-position of the 2,2'-bipyridine ligand and imidazolium ring. Compared with catalyst **IL-BPZ1**, normally, the coordination of nitrogen atoms of the pyridine groups to the metal zinc ion leads to a slightly shift. Thus, the direct proofs implied the successful synthesis of catalyst.

To further evaluate the detailed structure of catalyst, the new-synthesized complex **IL-BPZ1**, the corresponding ligand **IL-BP1**, as well as the simple (2,2'-bipyridine)ZnBr₂ (denoted as **BPZ**) for comparison, were characterized by FT-IR spectra (4000-400 cm⁻¹, see **Fig. 3**) and far-IR spectra (400-100 cm⁻¹, see

Fig. 4). Firstly, the novel 2,2'-bipyridine ligand **IL-BP1**, without characteristic vibration bands in the far infrared region, displayed major characteristic bands around 1597 cm^{-1} , 1159 cm^{-1} , 619 cm^{-1} (**Fig. 3a**). After metalation, the characteristic bands in the FT-IR spectra of the novel complex **IL-BPZ1** appear as apparent blue shift from 1597 cm^{-1} , 1159 cm^{-1} , 619 cm^{-1} to 1618 cm^{-1} , 1167 cm^{-1} and 620 cm^{-1} , respectively, compared with those of the corresponding ligand **IL-BP1** (**Fig. 3a vs 3c**).

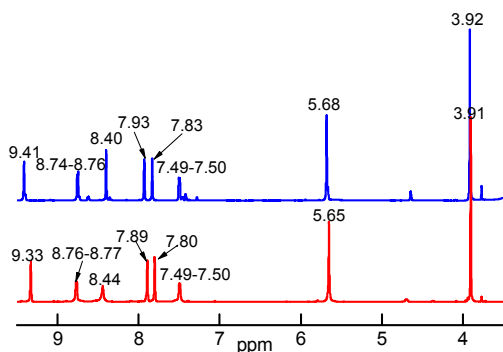


Fig. 2 The ^1H NMR results of catalyst **IL-BPZ1** (red line) and the corresponding ligand **IL-BP1** (blue line).

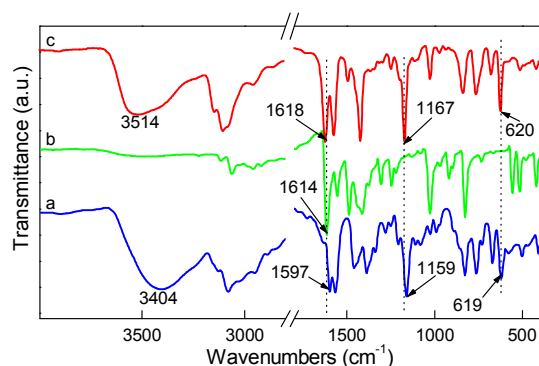


Fig. 3 The FT-IR spectra of ligand **IL-BP1**(a), catalyst **BPZ**(b) and **IL-BPZ1**(c).

Furthermore, the far-IR spectra of the novel complex **IL-BP1** shows new characteristic vibration bands at around 262 cm^{-1} and 206 cm^{-1} (**Fig. 4c**), which are associated with the stretching vibration modes of Zn-Br and Zn-N , respectively. These observations suggest that the 2,2'-bipyridine ligand could successfully coordinate with zinc ion through nitrogen atoms of the pyridine groups. Meanwhile, the IL-functionalized samples exhibited an additional feature at 1167 and 620 cm^{-1} assigned to the stretching vibration of characteristic peaks of imidazole fragment (**Fig. 3c vs 3b**).²⁴ The new stretching vibration further suggests the grafting of imidazolium IL moiety on the 2,2'-bipyridine ligand. In addition, compared to the far IR spectra of the neat complex **BPZ** ($\nu_{(\text{Zn-Br})}=248\text{ cm}^{-1}$, $\nu_{(\text{Zn-N})}=183\text{ cm}^{-1}$, see **Fig. 4b**), the blue-shift in the IR spectra of the novel complex **IL-BP1** ($\nu_{(\text{Zn-Br})}=262\text{ cm}^{-1}$, $\nu_{(\text{Zn-N})}=206\text{ cm}^{-1}$, see **Fig. 4c**) is mainly due to the electron-deficient substitutes of the imidazolium cations at the 4,4'-positions in the 2,2'-bipyridine ligands.²⁵

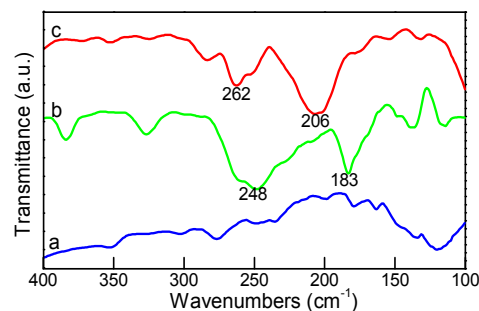


Fig. 4 The Far-IR spectra of ligand **IL-BP1**(a), catalyst **BPZ**(b) and **IL-BPZ1**(c).

Additionally, the UV-vis spectra of catalyst **IL-BPZ1** superimposed on that of the free ligand **IL-BP1** in water solution is reported in **Fig. 5**. The ligand **IL-BP1** and the corresponding zinc complex **IL-BPZ1** all typically shows two maximum absorption bands at 236 nm and 284 nm , attributed to $\pi-\pi^*$ spin-allowed transitions involving the aromatic rings.²⁶ Nevertheless, the UV-vis spectrum of a concentrated water solution of **IL-BPZ1** shows the presence of a broad band at around 490 nm that is missing in the absorption spectra of **IL-BPZ1** in dilute solution, which is due to the ligand-to-metal charge transfer transitions in the 2,2'-bipyridine Zn(II) complex. The observation implies that the active site (metal center) of the IL-functionalized 2,2'-bipyridine Zn(II) complex is maintained.

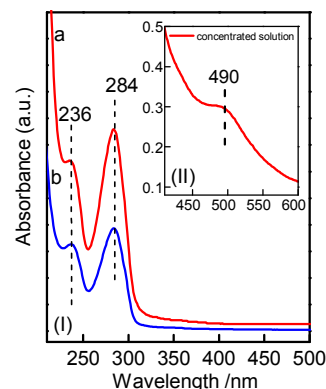


Fig. 5 (I) The UV-vis spectra of catalyst **IL-BPZ1** and the corresponding ligand **IL-BP1**; (II) The UV-vis spectra of a concentrated water solution of catalyst **IL-BPZ1**.

Thermal analysis was used to monitor the decomposition profiles of IL grafted complex of **IL-BPZ1**, and the obtained results are depicted in **Fig. 6**. The first obvious large loss in weight centres is at $345\text{ }^\circ\text{C}$. The thermo-stability of catalyst **IL-BPZ1** was obviously superior to the corresponding ligand **IL-BP1** (or **IL**) that the large loss weight centres was at $295\text{ }^\circ\text{C}$ ($312\text{ }^\circ\text{C}$ for **IL**, **Fig. 6a vs 6b, 6c**). As mentioned, this weight loss is logically assigned to the successive cleavage of 2,2'-bipyridine ligand. Notably, the temperature of the successive cleavage of the 2,2'-bipyridine ligand moieties in the **IL-BPZ1** gets increased up to $520\text{ }^\circ\text{C}$, due to the mutual stabilization of the 2,2'-bipyridine ligand part and the ILs moieties. It is indirect proof for the successful grafting of ILs moiety on the 2,2'-bipyridine ligand. The third weight loss appeared $520\text{ }^\circ\text{C}$ and was followed by an additional weight loss at $600\text{ }^\circ\text{C}$ which extended up to *ca.* $690\text{ }^\circ\text{C}$. The two steps were well distinguished in the

corresponding DTG curve (Fig. 6(B)). We tentatively assigned these steps to the complete decomposition of the ligand and ILs.²⁷ The non-removable residue belonged to the formation of zinc oxide in air atmosphere at high temperature.²⁴ It was indirect proof for the successful coordination to the 2,2'-bipyridine ligand using zinc salt with respect to the TG curve of ligand **IL-BP** or **IL**. According to TG-DTG data, the robust catalyst **IL-BPZ1** remains stable up to 250 °C.

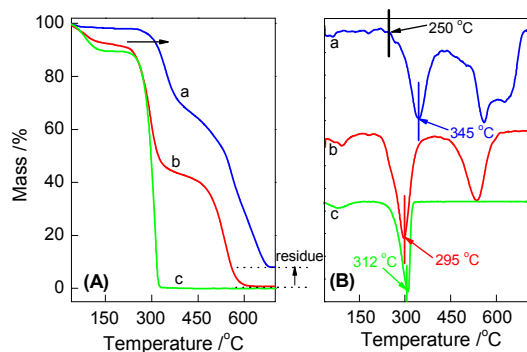


Fig. 6 Thermogravimetric TG (A) and differential thermogravimetric DTG (B) results of catalyst **IL-BPZ1** (a, blue line), ligand **IL-BP1** (b, red line) and **IL** (c, green line).

Effect of catalysts

The catalytic performances of the novel catalysts **IL-BPZ** were measured in the model cycloaddition reaction of allyl glycidyl ether (AGE) with CO₂, which was conducted in a semi-batch operation in the presence of the catalyst under mild conditions (0.5 mol%, 373 K, 1.0 MPa, 4 h, Table 1). In the absence of catalyst or the sole addition of ZnBr₂, even simple 2,2'-bipyridine ligand, the reaction does not proceed at all (Table 1, entry 1-3). While 1.0 mol% of the conventional ionic liquid **IL** (2 equiv.) could catalyse the cycloaddition reaction, the yield of allyl glycidyl carbonate (AGC) was very low (Table 1, entry 4) under solvent-free conditions. Note that simple 2,2'-bipyridine Zn(II) bromide complex (denoted as **BPZ**, see Chart 1), even **IL**-functionalized 2,2'-bipyridine ligand **IL-BP** without ZnBr₂ present poor catalytic performance under the given conditions (Table 1, entry 5-6). To our delight, 2,2'-bipyridine Zn(II) bromide complexes bearing various imidazolium-based **IL** units (**IL-BPZ**, Scheme 1), as a kind bi-functional complex, exhibit excellent catalytic performance. The catalytic performance with the employment of the catalyst **IL-BPZ1** is similar to that upon the binary catalyst system for a simple physical mixture of complex **BPZ** with **IL** using the molar ratio of 1:2 (Table 1, entry 7-8 vs entry 9).²⁸ This observation indicates **IL-BPZ1** bearing intramolecular nucleophilic co-catalyst acts as single-component catalyst to complete the catalytic cycle based on the acid-base synergistic catalytic mechanism.²⁹ Because the epoxide could be coordinated with the Lewis acidic site Zn to form the adduct of the metal-epoxide, then basic site Br⁻ anion of the **IL** makes a nucleophilic attack on the less hindered carbon atom of the coordinated epoxide followed by ring opening. Notably, the two-component catalytic system ZnBr₂/**IL-BPZ1** with equivalent molar ratio has low catalytic performance in the cycloaddition reaction (Table 1, entry 10). It suspects that adding both separate components together may require a small induction period to form in situ the **IL-BPZ1** system. When adding the substrate together with

the separate components other complexes based on the zinc reagent may form because of the kinetic effect. Thus, when the molar ratio increased to 2:1, the similar results were obtained with respect to the complex **IL-BPZ1** (Table 1, entry 11). Moreover, in the catalytic system, 92% yield of AGC could be obtained under even 1 atm CO₂ pressure for 12 h (Table 1, entry 12). Unfortunately, the coupling reaction could basically not occur under room temperature and atmospheric pressure even prolonged the reaction time to 72 h.

Table 1 The results of the cycloaddition reaction of AGE with CO₂ catalyzed by various catalysts.^a

Entry	Catalyst	Conv. ^b /%	Yield ^b /%	TOF ^c /h ⁻¹
1	-	-	-	-
2	ZnBr ₂	n. r.	n. r.	-
3	2,2'-bipyridine	n. d.	n. d.	-
4	IL	41	40	20
5	BPZ	11	8	4
6	IL-BP1	10	9	4.5
7	IL-BPZ1	85	84	42
8 ^d	IL-BPZ1	96	95	38
9 ^d	BPZ/IL (1:2)	95	93	37.2
10	ZnBr ₂ / IL-BP1 (1:1)	49	47	23.5
11	ZnBr ₂ / IL-BP1(2:1)	95	93	37.2
12 ^e	IL-BPZ1	93	92	15.3

^a Reaction conditions: 10 mL stainless-steel clave, AGE (6 mmol), catalyst (0.03mmol, 0.5 mol%), CO₂ pressure (1.0 MPa), reaction temperature (100 °C), reaction time (4 h);
^b Determined by GC using biphenyl as the internal standard;
^c Turnover frequency (TOF): mole of synthesized AGC per mole of catalyst per hour;
^d Reaction proceeded for about 5 h under identical conditions.
^e Reaction proceeded at 100 °C under 1 atm CO₂ pressure for about 12 h.

Effect of reaction parameters

The effect of temperature and pressure on the cycloaddition reaction is investigated. As expected, the reaction temperature had a positive effect on the catalytic reaction.³⁰ From Fig. 7(I), it can be seen that the yield of the AGC achieved 96 % when the reaction temperature was 100 °C. However, no significant difference was observed when temperature was increased to 110 °C. When the reaction was carried out at low temperature (e.g. 80 °C), much lower conversion of AGE (less than 11 %) was obtained. Moreover, because the gas-liquid diffusion between epoxide and CO₂ may have an effect on the reaction kinetics in the mass transfer, there are optimal ranges of CO₂ pressure for the maximum conversion of AGE. The pressure has a great effect on the conversion of AGE upon varying the CO₂ pressure in the range 0.1-1.0 MPa, whereas the conversion changes

only slightly in the range 1.0-3.0 MPa (see Fig. 7(II)). It indicated that higher CO₂ pressure enhanced AGC yield due to the higher CO₂ concentration in the liquid phase of the reaction system under a low-pressure region.³¹ The results demonstrated that this catalytic system could be operated with high efficiency under mild conditions (100 °C, 1.0 MPa). Thus, the effect of the amount of catalyst on the cycloaddition was also examined (see Fig. 7(III)). The results indicated that the catalyst amount had significant impact on the reactions. The conversion of AGE significantly increased with enhancement of the amount of catalyst under the same reaction conditions (from 0.1 to 0.5 mol %). When the using amount of catalyst was further increased up to 0.75 mol%, the AGC conversion by only a small margin was obtained.^{7a} In addition, the dependence of the AGE conversion on reaction time at the identical conditions was presented in Fig. 7(IV). It can be seen that the conversion of AGE increased rapidly with the reaction time and that nearly all the AGE could be converted within 6 h. It should be noted that the selectivity towards the desired AGC was essentially 99 %, since GC-MS analysis and ¹H NMR showed that there were no other detectable products.

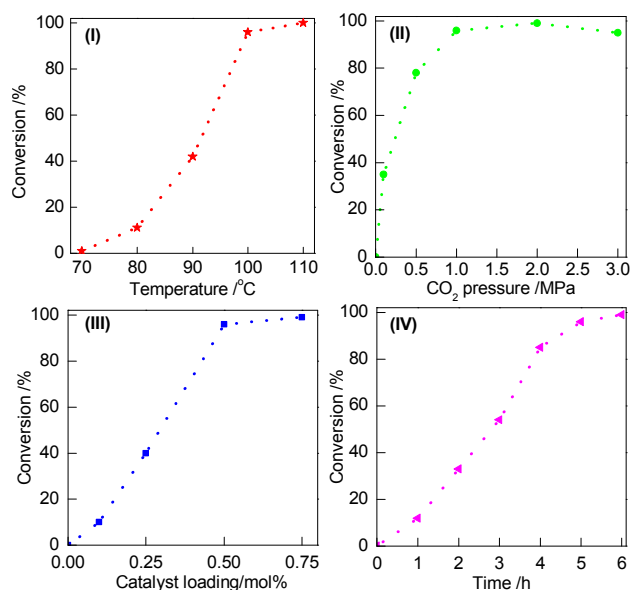


Fig. 7 Optimization of reaction conditions with catalyst **IL-BPZ1**; reaction conditions: 10 mL stainless-steel clave, AGE (6 mmol), (I) CO₂ pressure (1.0 MPa), 5 h, 0.5 mol% catalyst; (II) temperature (100 °C), 0.5 mol% catalyst, 5 h; (III) temperature (100 °C), CO₂ pressure (1.0 MPa), 5 h; (IV) temperature (100 °C), CO₂ pressure (1.0 MPa), 0.5 mol% catalyst.

Effect on the various structures of the catalysts

Under the optimal conditions, we further evaluated the effect on the different structures of the catalyst on the coupling reaction of AGE to CO₂. Initially, the catalytic activity of catalysts **IL-BPZ** was affected by the chain length of the substituent in N-position of the imidazolium ring. As shown in Fig. 8, **IL-BPZ** series catalysts with longer alkyl side chains were proved the observed higher activity (**IL-BPZ2** or **IL-BPZ3** vs **IL-BPZ1**). The AGE conversion increased with the length of the alkyl chain increased from methyl to *n*-butyl, further to *n*-octyl. It can be assumed that the bulkiness of the alkyl imidazolium cation forces the bromide ion away from the

cation, and this weaker electrostatic interaction would render the anion more nucleophilic. Therefore, they were more effective in nucleophilic attack of the anion to the oxirane ring of AGE.³² More importantly, **IL-BPZ4** bearing three EO units exhibited the highest activity with respect to **IL-BPZ3** owing the identical hydrophobic alkyl chain length, which was also shown by our group's previous work.¹⁶ The phenomenon could be attributed to "CO₂-expansion" effect of PEO chains, which was originated from the weak interaction between the CO₂ molecule and the PEO chain.

Furthermore, the nature of halide groups bonded to the zinc center also significantly affected the catalytic activity (see Fig. 8(II)). When the Lewis acidity of the metal cation is stronger, the coordination of the epoxide is easier. In addition, a more nucleophilic anion is favourable for its interaction with the carbon atom of CO₂.²⁹ Therefore, the conversion of the AGC increased with the increasing nucleophilicity and the leaving ability of halide ion (I⁻>Br⁻>Cl⁻).^{28,33} On the basis of this result, it could be suggested that the leaving ability was beneficial to increasing catalytic activity. Additionally, the reactions also depend greatly on the kind of counter anions of imidazolium-based IL moieties in the catalysts (**IL-BPZ1** vs **IL-BPZ6**). These results illuminate that the counter ions play an important role in the catalytic activity and the Br⁻ is the most effective of these negative ions for the cycloaddition reaction of AGE with CO₂. The activity of Br⁻ was higher than BF₄⁻, in which is consistent with the order of the nucleophilicity of the anions. Thus, these results indicate that non-nucleophilic nature of BF₄⁻ anion is not favourable components for the coupling reaction, which leads to a lower conversion of the epoxide.³⁴ The rate determining step of the epoxide-CO₂ reaction involves nucleophilic attack of the bromide anion to AGE. More nucleophilic anion will more easily attack the epoxide ring to form reaction intermediate. Additionally, the most common nitrogen containing organic cations within IL units are imidazolium and pyridinium derivatives. Fig. 8(IV) shows that the relationship between type of onium cation in IL units and the activity of the catalysts (**IL-BPZ1** vs **IL-BPZ8**). The catalytic activity on the coupling reaction decreases in the order of imidazolium>pyridinium, which hints the incorporation of the imidazolium group within the 2,2'-bipyridine ligand is beneficial for catalytic performance.³⁵

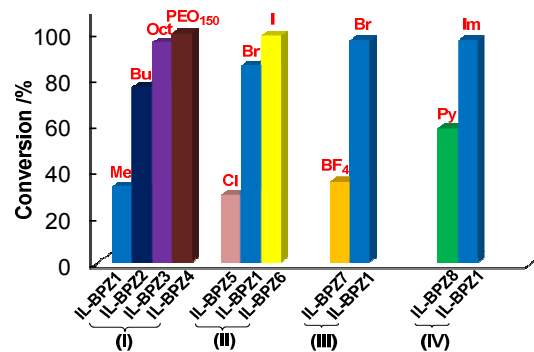


Fig. 8 The reactivity of various catalysts with different structures for the cycloaddition reaction of AGE with CO₂; reaction conditions: 10 mL stainless-steel clave, AGE (6 mmol), temperature (100 °C), CO₂ pressure (1.0 MPa), 0.5 mol% catalyst; (I) 2 h; (II) 4 h; (III-IV) 5 h.

Catalytic activity towards other epoxides

To survey the scope of substrates, we examined the cycloaddition reactions of other commercially available epoxides (such as propylene oxide (PO), 1,2-epoxybutane, epichlorohydrin (ECH), styrene oxide (SO) and its derivatives) with CO₂ by performing the reaction with 0.5 mol% catalyst **IL-BPZ1** under the identical conditions (1.0 MPa, 100 °C, 5 h) as elaborated in **Table 2**. Obviously, most terminal epoxide substrates (**1a-e**) could be smoothly converted to corresponding cyclic carbonates with high conversion and excellent selectivity (**Table 2**, entries 1-5). The activity of epoxides decreased as the alkyl length increasing (entry 1 vs entry 2). Moreover, for bromo or chloro-substituted SO derivatives (such as **1g** and **1h** with electron-withdrawing substituents on the *para*-position of aromatic ring), the yields are generally lower than those with electron-donating substituents (e.g. methyl group **1e**). It suggested that for SO and its derivatives the nucleophilic ring-opening occurs mainly at the α -carbon of the epoxide ring due to a consequence of the electron-withdrawing inductive effect of the phenyl group (**Table 2**, entry 6 vs entries 5, 7-8).^{2f} Similarly, the electron-withdrawing nature of the chloromethyl group of ECH tends to drive the reaction towards the cyclic carbonate product (**Table 2**, entry 3). Unfortunately, the internal epoxide, cyclohexene oxide (CHO), exhibited lower activity (**Table 2**, entry 9) presumably due to the high steric hindrance. This steric effect was more likely to hinder the nucleophilic attack of the epoxide rather than its coordination to the Lewis acid metal center. Thus, both steric and electronic effects play an important role on the chemical coupling reaction of epoxide and CO₂.³⁶

Table 2 The results of the coupling reaction of CO₂ to various epoxide substrates over the **IL-BPZ1**.^a

Entry	Epoxide	Product	Conv. ^b %	Yield ^b %
1			>99	99
2			95	93
3			99	98
4			96	95
5			93	90
6			88	85
7			65	61
8			28	25
9			3	<1

8			28	25
9			3	<1

^a Reaction conditions: 10 mL stainless-steel clave, epoxide (6 mmol), **IL-BPZ1** (0.03mmol), reaction temperature (100 °C), reaction time (5 h), CO₂ pressure (1.0 MPa), product identification via FT-IR, ¹H NMR, ¹³C NMR and GC-MS;

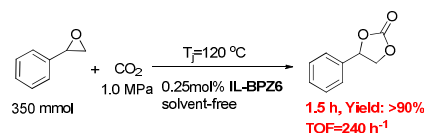
^b Same as **Table 1**.

Recycling of the Catalyst

A series of catalytic recycles were carried out to test the stability and reusability of the catalyst under the optimized conditions. In each cycle, the cyclic carbonate product was easily extracted with ethyl acetate or ether then the catalyst was precipitated after centrifugation. Subsequently, the solid precipitation was filtrated, washed with Et₂O and dried in vacuum and was reused in the subsequent reactions. The yields of the product obtained from the second (95%), third (92%), and fourth runs (90%) were similar to those obtained with the fresh catalyst under the identical conditions. Accordingly, the IL-catalyst could be reused at least four times with only a slight loss of catalytic activity, consistent with only a slight leaching of the active catalyst species. Therefore, the special solubility of the complexes endows them with the feature of solvent-regulated separation.

Large-scale synthesis of styrene cyclic carbonate

In view of the easy operation and analysis, we choose styrene oxide (SO, b.p.=191 °C) as a model substrate to apply the large-scale synthesis of SC using Mettler Toledo EasyMaxTM102 system equipped with a 100 mL stainless steel autoclave in a semi-batch operation (CO₂ was continuously supplied to the reactor). The course of reaction was also monitored by the *in situ* IR spectroscopy.



Scheme 2 The results of the large-scale synthesis of SC.

As shown Scheme 2, the >90 % yield of SC was obtained with **IL-BPZ6** at 120 °C (keep Jacket temperature T_j constant) without solvent, while the TOF value reach up to 240 h⁻¹. Meanwhile, from the results of *in situ* IR spectra, the intensity of the characteristic peak for SO at 876 cm⁻¹ and 815 cm⁻¹ (epoxy ring skeleton vibration) declined rapidly, whereas an increasing intensity of the signals at 1159 cm⁻¹, 1065 cm⁻¹ (asymmetrical C-O vibration) and the peak around 1810 cm⁻¹ (C=O stretching vibration) indicated the formation of SC as the sole product (see **Fig. 10**). The results suggest that the homogenous catalyst could maintain the high catalytic activity with excellent selectivity in large-scale production.

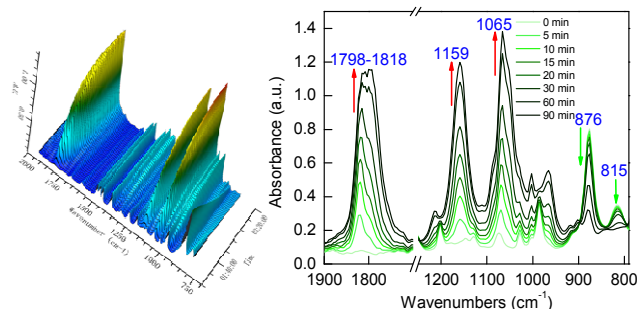


Fig. 10 (I) Three-dimensional stack plot of IR spectra collected every 1 min during the coupling reaction of SO and CO₂ with 0.25 mol% **IL-BPZ6** at 120 °C (T₁) and 1.0 MPa CO₂ pressure without solvent; (II) Decreases of the epoxide ring vibrational modes with a concomitant increase of the SC peaks at different times.

Additionally, it was also noted that reactions carried out at the low concentration (0.25 mol% **IL-BPZ1** or **IL-BPZ6**) had an induction period under solvent-free conditions. Meanwhile, we found that the induction period could be shortened following the increased reaction temperature (**Fig. 11a** vs **Fig. 11b**). Especially, catalyst **IL-BPZ6** has shorter induction period due to the better solubility with respect to **IL-BPZ1** (**Fig. 11b** vs **Fig. 11c**) in CO₂-epoxide mixture under identical conditions. Furthermore, if adding propylene carbonate as solvent, the induction period disappeared since catalyst **IL-BPZ** could be dissolved fully in the beginning stage (**Fig. 12-13**).

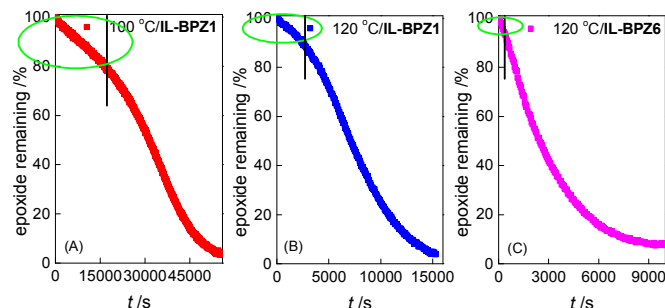


Fig. 11 Decrease in SO mole concentration with time with catalyst **IL-BPZ1** or **IL-BPZ6** (0.25 mol%) under solvent-free condition at 100 °C-120 °C (T₁) and 1.0 MPa CO₂ pressure (the green circle represents the reaction induction period).

Kinetics studies and mechanistic considerations

To investigate the mechanism of cyclic carbonate synthesis, a study of the reaction kinetics was undertaken as depicted in Eq. 1-8 (the general form of rate equation). From the *in situ* IR spectra, the data were found to fit to the following rate equations: [SO], [CO₂] and [Cat] are the SO, CO₂ and catalyst concentrations respectively; a, b and c are the order of reaction; t is time and k_{obs} is the observed pseudo-first-order rate constant for SO conversion (Eq. 1).

$$\text{Rate} = k[\text{SO}]^a[\text{CAT}]^b[\text{CO}_2]^c \quad \text{Eq. 1}$$

$$\text{Rate} = k_{\text{obs}}[\text{SO}]^a \quad \text{Eq. 2}$$

$$\text{Rate} = -d[\text{SO}]/dt \quad \text{Eq. 3}$$

$$-\ln[\text{SO}] = k_{\text{obs}}t \quad \text{Eq. 4}$$

$$\text{Rate} = k_{\text{obs}}[\text{SO}]^1 \quad \text{Eq. 5}$$

$$\text{Rate} = k'_{\text{obs}}[\text{CAT}]^b \quad \text{Eq. 6}$$

$$\ln \text{Rate} = \ln k'_{\text{obs}} + b \ln [\text{CAT}] \quad \text{Eq. 7}$$

$$\text{Rate} = k'_{\text{obs}}[\text{CAT}]^2 \quad \text{Eq. 8}$$

Firstly, it can be assumed that the concentrations of catalyst are constant during reaction and CO₂ is present in large excess due to the semi-batch operation so that b=c=0 (Eq. 2). Thus, in the event, the observed rate constant was determined from the slope of a linear plot of the natural logarithm of the changing sample concentration with time at different temperatures (Eq. 3-4). **Fig. 12-13** shows the determination of the observed rate constant for SO conversion by the catalyst **IL-BPZ1** at 100 °C using propylene carbonate (PC) as solvent. It was repeated for the other reaction temperatures and catalyst compositions. All the kinetic experiments showed a good fit to first order kinetics, implies that the reactions are first order in SO (Eq. 5).

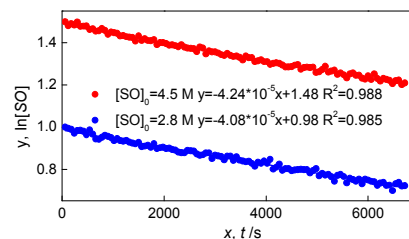


Fig. 12 Pseudo-first order kinetic plot of the natural logarithm of different SO concentration against time for the **IL-BPZ1** (0.14 mol%) at 100 °C (T₁) and 1.0 MPa CO₂ pressure using PC as solvent.

Furthermore, assuming steady state conditions at the beginning of the reaction, and thus CO₂ and SO concentrations are more or less constant. The rate law for this process may be rewritten as Eq. 6, in which k'_{obs} represents the rate constant, b is the order of reaction and [CAT] is the concentration of **IL-BPZ1**. Then, by taking the natural logarithm of Eq. 6, Eq. 7 is obtained. The kinetic data was fitted by the natural logarithm of the observed pseudo-first order rate constant (ln k'_{obs}) against the natural logarithm of the catalyst concentrations (ln [CAT]) (Eq. 7). The logarithmic plot revealed that b is close to 2.0 suggesting the reaction is second order in the single-component catalyst **IL-BPZ1** (Eq. 7, see **Fig. 13**).

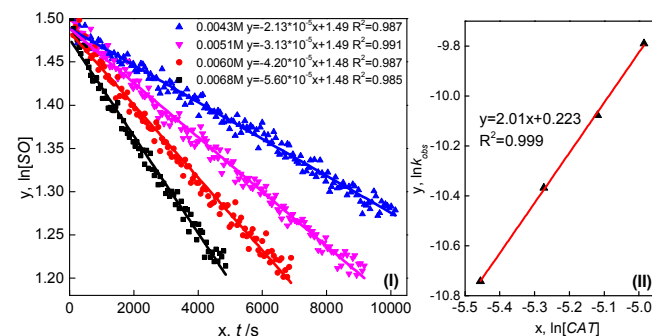


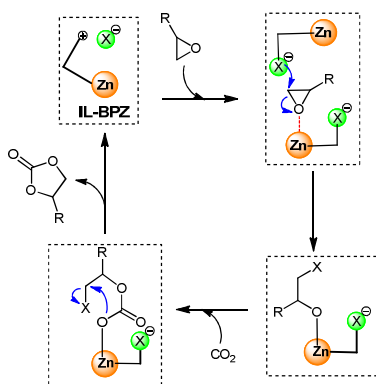
Fig. 13 (I) Decrease in SO mole concentration ([SO]₀ = 4.5 M, 21 g) with time with catalyst **IL-BPZ1** (0.0043-0.0068 M) in PC (21 g) at 100 °C (T₁) and 1.0 MPa CO₂ pressure; (II) The fitting curve of the natural logarithm of the observed pseudo-first order rate constant (ln k'_{obs}) against the natural logarithm of the catalyst concentration (ln [CAT]).

Based on the molecule structure of the complex **IL-BPZ** and the cycloaddition reaction results, a possible mechanism of the acid-base synergetic catalysis for cyclic carbonate synthesis is also proposed, which is similar to our previous work.¹⁶ The kinetic study hints bimetallic pathway involving two separated monometallic

complexes has been inspired for the ring opening of epoxides (Scheme 3). This intermolecular mechanism is similar to the monometallic pathway,¹⁶ but there is the difference that the nucleophile X^- is coordinated to a metal centre, and it also attacks the epoxide activated by the second metal centre. This pathway is expected to occur when low catalyst/epoxide ratios are employed.^{2f} Further experiments are in progress to elucidate the reaction mechanism.

Conclusions

Several 2,2'-bipyridine zinc(II) complexes functionalized by imidazolium based ILs were first prepared and used as catalysts for the cycloaddition reaction of CO_2 and various epoxides to provide cyclic carbonate under quite mild conditions. The catalyst of **IL-BPZA** with longer PEO chain showed the best catalytic activity, which afforded AGC in 98% yield and 99% selectivity within 2 h under 100 °C and 1.0 MPa CO_2 pressure conditions. The cooperative action mechanism for ring-opening of the epoxide between an anion X^- within ILs and a metal center was proposed. In addition, the reaction kinetic data *via* the *in situ* IR spectroscopy revealed that the reaction was first-order with respect to epoxide and second-order for catalyst at the low concentration range.



Scheme 3 The plausible mechanism for the coupling reaction with the IL-BPZ.

Experimental Section

Reagents and Methods: Propylene oxide (PO), propylene carbonate (PC), epichlorohydrin (ECH), allyl glycidyl ether (AGE), styrene oxide (SO), zinc bromide, 1-methylimidazole, sodium fluoroborate and 4-methylpyridine were obtained by J&K Scientific Ltd. 4-chlorostyrene oxide and 4-bromostyrene oxide was purchased from Alfa Aesar Chemical Reagent Co. Ltd. Zinc chloride was produced by Acros Organics. Sodium borohydride, zinc iodide, 4,4'-dimethyl-2,2'-dipyridyl and 2,2'-bipyridyl-4,4'-dicarbonyl acid were received from Energy Chemical. 1-butylimidazole and 1-octylimidazole were bought from TCI. Other commercially available chemicals were laboratory grade reagents from local suppliers. CO_2 was purified by passing through a column packed with 4A molecule sieves before use (99.99%). All of the solvents were purified by standard procedures.³⁷ 4-methylstyrene oxide was prepared using the Jacobsen's catalyst.²⁴ 4,4'-dibromomethyl-2,2'-bipyridine was synthesized according to the reported literature (see ESI).²²

FT-IR spectra were obtained as potassium bromide pellets with a resolution of 4 cm^{-1} and 32 scans in the range 400-4000 cm^{-1} using a

Bruker spectrophotometer. The ultraviolet-visible light (UV-vis) spectra were recorded on a Shimadzu UV2450 spectrophotometer. The solution of samples in ultrapure water (*ca.* 1.0 mM) was poured into a 1 cm quartz cell for UV-vis adsorption with ultrapure water as the reference. 1H NMR and ^{13}C NMR spectra were recorded on a Bruker Avance III 400 M spectrometer. The thermogravimetric and differential thermogravimetric (TG-DTG) curves were obtained on a NETZSCHSTA 449C thermal analyser. Samples were heated from room temperature up to 700 °C under flowing air using alumina sample holders. The sample weight was *ca.* 10 mg and the heating rate was 10 K min^{-1} . The conversions and yields of cyclic carbonate products were measured by a GC2010 gas chromatograph (Shimadzu) equipped with the capillary column (Rtx-5, 30m \times 0.32mm \times 0.25 μ m) and the FID detector. The course of reaction for kinetic study was also monitored by the *in situ* IR spectroscopy using a Mettler Toledo React IR ic10 reaction analysis system with DiComp ATR probe (Diamond, AgX 6mm \times 1.5m Fiber). In this manner, a single 256-scan background spectrum was collected. The infrared spectrometer was set up to collect one spectrum every 1 min over 24 hour. Profiles of the absorbance at 815 cm^{-1} with time were recorded and used to provide initial reaction rates for analysis.^{11b, 38} The cycloaddition reaction of epoxides with CO_2 was carried out according to the recently-published reference and NMR characterizations of the typical cyclic carbonate products (**2a-i**) were also listed in the literature¹⁶.

General Procedure for the Synthesis of various ionic liquid functionalized 2,2'-bipyridine zinc(II) complex

Synthesis of bis(1-methyl-3-methyleneimidazolium bromine) modified 2,2'-bipyridine: N-methylimidazole (0.821 g, 10 mmol) in dry toluene (100 mL) was added dropwise into the stirring toluene solution of 4,4'-dibromomethyl-2,2'-bipyridine (1.71 g, 5 mmol)²² under nitrogen atmosphere. The reaction was heated to reflux for 12 h. After cooling, the solvent was evaporated in vacuo and the lower viscous liquid was washed three times with dry benzene (3 \times 20 mL) and ether (3 \times 50 mL), respectively. The solvent was removed to obtain the compound **IL-BP** as the viscous liquids. Yield: 92 %. Ligands **IL-BP2**, **IL-BP3** and **IL-BP4** were also prepared using 1-butylimidazole, 1-octylimidazole and N-(polyoxyethylene methyl ether)imidazole,¹⁶ instead of N-methyl imidazole, respectively. **IL-BP1:** FT-IR (KBr), γ_{max}/cm^{-1} : 3405, 3079, 1597, 1566, 1459, 1387, 1338, 1279, 1206, 1160, 1108, 1080, 1024, 990, 825, 762, 729, 670, 620, 577, 501; 1H NMR (400 MHz, D_2O) δ_H =8.54-8.56 (d, J=8 Hz, 2H), 7.89 (s, 2H), 7.46-7.48 (d, J=8 Hz, 4H), 7.34-7.35 (d, J=4Hz, 2H), 5.52 (s, 4H), 3.87 (s, 6H); ^{13}C NMR (100.4 MHz, D_2O) δ_C =155.47, 149.92, 145.33, 136.85, 124.29, 123.37, 122.71, 120.91, 51.42, 35.99.

Synthesis of bis(1-methyl-3-methyleneimidazolium bromine) modified 2,2'-bipyridine Zn(II) complex: Zinc bromine (2.5 mmol) dissolved in 100 mL anhydrous ethanol was added dropwise into the stirring absolute ethanol solution of above-obtained 2,2'-bipyridine ligand (1.26 g, 2.5 mmol) under nitrogen atmosphere. Abundant white precipitate was emerged immediately, and then the reaction was heated to reflux for 12 h. After cooling, the white solid product was collected and washed thoroughly with ethanol (3 \times 20 mL). **IL-BPZI** (Yield, 86 %): FT-IR (KBr), γ_{max}/cm^{-1} : 3514, 3101, 1618, 1569, 1489, 1418, 1243, 1166, 1021, 833, 759, 673, 620, 508, 1H NMR(400 MHz, $DMSO-d_6$) δ_H =9.33(s, 2H), 8.76-8.77(d, 2H), 8.44(s, 2H), 7.89(s, 2H), 7.80(s, 2H), 7.49-7.50(d, 2H), 5.65(s, 4H), 3.91(s, 6H); ^{13}C NMR (100.4 MHz, $DMSO-d_6$) δ_C =150.46, 137.75, 124.74, 124.03, 123.11, 120.28, 51.18,

36.55. ESI-MS: $m/z=651$ (M-Br)⁺; The other catalysts **IL-BPZ2-8** were also prepared following the similar procedure. **IL-BPZ2**(Yield, 80 %): FT-IR (KBr), $\gamma_{\max}/\text{cm}^{-1}$: 3441, 3068, 2958, 2931, 2867, 1616, 1563, 1489, 1416, 1364, 1243, 1194, 1159, 1021, 834, 749, 640, 508; ¹H NMR(400 MHz, DMSO-*d*₆) $\delta_{\text{H}}=9.43(\text{s}, 2\text{H}), 8.76-8.77(\text{d}, 2\text{H}), 8.39(\text{s}, 2\text{H}), 7.92(\text{s}, 4\text{H}), 7.48-7.49(\text{d}, 2\text{H}), 5.65(\text{s}, 4\text{H}), 4.22-4.25(\text{t}, 4\text{H}), 1.79-1.83(\text{t}, 4\text{H}), 1.24-1.33(\text{m}, 4\text{H}), 0.89-0.93(\text{t}, 6\text{H})$; ¹³C NMR (100.4 MHz, DMSO-*d*₆) $\delta_{\text{C}}=150.47, 137.25, 123.94, 123.56, 123.41, 119.98, 51.34, 49.34, 31.68, 19.26, 13.79$; ESI-MS: $m/z=735$ (M-Br)⁺; **IL-BPZ3** (Yield, 90 %): FT-IR (KBr), $\gamma_{\max}/\text{cm}^{-1}$: 3445, 3134, 3071, 2927, 2856, 1619, 1565, 1419, 1368, 1243, 1160, 1023, 835, 745, 641, 509; ¹H NMR(400 MHz, DMSO-*d*₆) $\delta_{\text{H}}=9.39(\text{s}, 2\text{H}), 8.71-8.73(\text{d}, 2\text{H}), 8.37(\text{s}, 2\text{H}), 7.88(\text{s}, 4\text{H}), 7.45(\text{s}, 2\text{H}), 5.62(\text{d}, 4\text{H}), 4.18-4.21(\text{s}, 4\text{H}), 1.78-1.81(\text{s}, 4\text{H}), 1.19-1.23(\text{s}, 24\text{H}), 0.79-0.82(\text{s}, 6\text{H})$; ¹³C NMR (100.4 MHz, DMSO-*d*₆) $\delta_{\text{C}}=151.80, 147.20, 138.58, 125.30, 124.91, 124.76, 121.46, 63.39, 52.72, 50.99, 41.83, 41.62, 41.41, 41.20, 32.93, 31.03, 30.25, 30.10, 27.41, 27.29, 23.84, 15.74$; ESI-MS: $m/z=847$ (M-Br)⁺; **IL-BPZ4**(Yield, 80 %): FT-IR (KBr), $\gamma_{\max}/\text{cm}^{-1}$: 3423, 3112, 2911, 1617, 1565, 1523, 1490, 1417, 1354, 1291, 1241, 1159, 1099, 1024, 948, 835, 762, 657, 512; ¹H NMR(400 MHz, DMSO-*d*₆) $\delta_{\text{H}}=9.35(\text{s}, 2\text{H}), 8.68-8.75(\text{d}, 2\text{H}), 8.43(\text{s}, 2\text{H}), 7.99(\text{s}, 2\text{H}), 7.91(\text{s}, 2\text{H}), 7.48-7.59(\text{d}, 2\text{H}), 5.67(\text{s}, 4\text{H}), 4.68(\text{s}, 2\text{H}), 4.41(\text{s}, 2\text{H}), 3.37(\text{s}, 8\text{H}), 3.21(\text{s}, 3\text{H})$; ESI-MS: $m/z=551, 595, 639, 683, 727, 771$ (M-Br)⁺; **IL-BPZ5**(Yield, 89 %): FT-IR (KBr), $\gamma_{\max}/\text{cm}^{-1}$: 3486, 3103, 1618, 1569, 1489, 1418, 1364, 1242, 1166, 1095, 1020, 923, 833, 760, 673, 620, 507; ¹H NMR(400 MHz, DMSO-*d*₆) $\delta_{\text{H}}=9.30(\text{s}, 2\text{H}), 8.75-8.76(\text{d}, 2\text{H}), 8.41(\text{s}, 2\text{H}), 7.89(\text{s}, 2\text{H}), 7.79(\text{s}, 2\text{H}), 7.46-7.47(\text{d}, 2\text{H}), 5.63(\text{s}, 4\text{H}), 3.90(\text{s}, 6\text{H})$; ¹³C NMR (100.4 MHz, DMSO-*d*₆) $\delta_{\text{C}}=150.50, 137.74, 124.74, 123.87, 123.12, 120.16, 51.24, 36.53$; ESI-MS: $m/z=561$ (M-Br)⁺; **IL-BPZ6**(Yield, 86 %): ¹H NMR(400 MHz, DMSO-*d*₆) $\delta_{\text{H}}=9.34(\text{s}, 2\text{H}), 8.80(\text{s}, 2\text{H}), 8.66(\text{s}, 2\text{H}), 7.90(\text{s}, 2\text{H}), 7.82(\text{s}, 2\text{H}), 7.56-7.64(\text{m}, 2\text{H}), 5.70(\text{s}, 4\text{H}), 3.92(\text{s}, 6\text{H})$; ESI-MS: $m/z=745$ (M-Br)⁺; **IL-BPZ7**(Yield, 81 %): FT-IR (KBr), $\gamma_{\max}/\text{cm}^{-1}$: 3419, 3100, 1618, 1569, 1489, 1417, 1365, 1296, 1242, 1168, 1033, 833, 760, 672, 619, 514; ¹H NMR(400 MHz, DMSO-*d*₆) $\delta_{\text{H}}=9.30(\text{s}, 2\text{H}), 8.77(\text{s}, 2\text{H}), 8.46(\text{s}, 2\text{H}), 7.88(\text{s}, 2\text{H}), 7.79(\text{s}, 2\text{H}), 7.49-7.50(\text{d}, 2\text{H}), 5.65(\text{s}, 4\text{H}), 3.91(\text{s}, 6\text{H})$; ¹³C NMR (100.4 MHz, DMSO-*d*₆) $\delta_{\text{C}}=150.41, 137.78, 124.74, 122.98, 51.21, 36.53$; ESI-MS: $m/z=665$ (M-Br)⁺; **IL-BPZ8**(Yield, 92%): FT-IR (KBr), $\gamma_{\max}/\text{cm}^{-1}$: 3440, 3047, 1638, 1568, 1514, 1475, 1416, 1368, 1303, 1240, 1204, 1020, 924, 826, 769, 701, 629, 483; ¹H NMR(400 MHz, DMSO-*d*₆) $\delta_{\text{H}}=9.11-9.17(\text{m}, 4\text{H}), 8.73-8.78(\text{m}, 2\text{H}), 8.05-8.13(\text{m}, 4\text{H}), 7.52-7.53(\text{m}, 2\text{H}), 5.94-5.99(\text{s}, 2\text{H}), 2.62-2.68(\text{t}, 6\text{H})$; ESI-MS: $m/z=673$ (M-Br)⁺.

Acknowledgements

This work was supported by the National Natural Science Foundation of China (No. 21376278; 21276052; 21176267; 21036009). The authors are also thankful to University of Science and Technology of China for providing the help of far-IR spectra testing.

Notes and references

*School of Chemistry and Chemical Engineering, Key Laboratory of Low-Carbon Chemistry & Energy Conservation of Guangdong Province, Sun Yat-sen University, Guangzhou 510275, P.R. China. Email address: jihb@mail.sysu.edu.cn (H.B. Ji); Tel.: +86 20 84113658; Fax: +86 20 84113654.

- (a)T. Sakakura, J. C. Choi and H. Yasuda, *Chem. Rev.*, 2007, **107**, 2365-2387; (b)I. Omae, *Coordin. Chem. Rev.*, 2012, **256**, 1384-1405; (c)Z. Z. Yang, L. N. He, J. Gao, A. H. Liu and B. Yu, *Energy Environ. Sci.*, 2012, **5**, 6602-6639.
- (a)W. L. Dai, S. L. Luo, S. F. Yin and C. T. Au, *Appl. Catal. A: Gen.*, 2009, **366**, 2-12; (b)T. Sakakura and K. Kohno, *Chem. Commun.*, 2009, **47**, 1312-1330; (c)A. Decortes, A. M. Castilla and A. W. Kleij, *Angew. Chem.*, 2010, **51**, 10016-10032; *Angew. Chem. Int. Ed.*, 2010, **49**, 9822-9837; (d)M. North, R. Pasquale and C. Young, *Green Chem.*, 2010, **12**, 1514-1539; (e)J. Zhang, J. Sun, X. Zhang, Y. Zhao and S. Zhang, *Greenh. Gases: Sci. Technol.*, 2011, **1**, 142-159; (f)P. P. Pescarmona and M. Taherimehr, *Catal. Sci. Tech.*, 2012, **2**, 2169-2187.
- (a)A. A. G. Shaikh and S. Sivaram, *Chem. Rev.*, 1996, **96**, 951-976; (b)B. Schäffner, F. Schäffner, S. P. Verevkin and A. Börner, *Chem. Rev.*, 2010, **110**, 4554-4581; (c)H. Zhang, H. B. Liu and J. M. Yue, *Chem. Rev.*, 2013, **114**, 883-898.
- (a)T. Yano, H. Matsui, T. Koike, H. Ishiguro, H. Fujihara, M. Yoshihara and T. Maeshima, *Chem. Commun.*, 1997, **12**, 1129-1130; (b)K. Yamaguchi, K. Ebitani, T. Yoshida, H. Yoshida and K. Kaneda, *J. Am. Chem. Soc.*, 1999, **121**, 4526-4527.
- (a)V. Calo, A. Nacci, A. Monopoli and A. Fanizzi, *Org. Lett.*, 2002, **4**, 2561-2563; (b)T. Takahashi, T. Watahiki, S. Kitazume, H. Yasuda and T. Sakakura, *Chem. Commun.*, 2006, **15**, 1664-1666; (c)T. Sakai, Y. Tsutsumi and T. Ema, *Green Chem.*, 2008, **10**, 337-341; (d)B. Chatelet, L. Joucla, J. P. Dutasta, A. Martinez, K. C. Szeto and V. Dufaud, *J. Am. Chem. Soc.*, 2013, **135**, 5348-5351.
- (a)J. L. Song, Z. F. Zhang, B. X. Han, S. Q. Hu, W. J. Li and Y. Xie, *Green Chem.*, 2008, **10**, 1337-1341; (b)S. G. Liang, H. Z. Liu, T. Jiang, J. L. Song, G. Y. Yang and B. X. Han, *Chem. Commun.*, 2011, **47**, 2131-2133; (c)J. Ma, J. Liu, Z. Zhang and B. Han, *Green Chem.*, 2012, **14**, 2410-2420; (d)J. Tharun, G. Mathai, A. C. Kathalikkattil, R. Roshan, J. Y. Kwak and D. W. Park, *Green Chem.*, 2013, **15**, 1673-1677; (e)S. Kumar and S. L. Jain, *Ind. Eng. Chem. Res.*, 2013, **53**, 541-546; (f)K. R. Roshan, A. C. Kathalikkattil, J. Tharun, D. W. Kim, Y. S. Won and D. W. Park, *Dalton Trans.*, 2014, **43**, 2023-2031.
- (a)Z. Z. Yang, L. N. He, C. X. Miao and S. Chanfreau, *Adv. Synth. Catal.*, 2010, **352**, 2233-2240; (b)Z. Z. Yang, Y. N. Zhao, L. N. He, J. Gao and Z. S. Yin, *Green Chem.*, 2012, **14**, 519-527; (c)A. L. Girard, N. Simon, M. Zanatta, S. Marmitt, P. F. B. Goncalves and J. Dupont, *Green Chem.*, 2014, **16**, 2815-2825; (d)J. Q. Wang, W. G. Cheng, J. Sun, T. Y. Shi, X. P. Zhang and S. J. Zhang, *RSC Advances*, 2014, **4**, 2360-2367; (e)M. H. Anthofer, M. E. Wilhelm, M. Cokoja, I. I. E. Markovits, A. Pothig, J. Mink, W. A. Herrmann and F. E. Kuhn, *Catal. Sci. Tech.*, 2014, **4**, 1749-1758.
- (a)H. S. Kim, J. J. Kim, B. G. Lee, O. S. Jung, H. G. Jang and S. O. Kang, *Angew. Chem.*, 2000, **112**, 4262-4264; *Angew. Chem. Int. Ed.*, 2000, **39**, 4096-4098; (b)R. L. Paddock and S. T. Nguyen, *J. Am. Chem. Soc.*, 2001, **123**, 11498-11499; (c)X. B. Lu, Y. J. Zhang, K. Jin, L. M. Luo and H. Wang, *J. Catal.*, 2004, **227**, 537-541; (d)R. L.

- Paddock and S. T. Nguyen, *Chem. Commun.*, 2004, **14**, 1622-1623; (e)C. J. Whiteoak, E. Martin, M. M. Belmonte, J. Benet-Buchholz and A. W. Kleij, *Adv. Synth. Catal.*, 2012, **354**, 469-476; (f)C. J. Whiteoak, N. Kielland, V. Laserna, E. C. Escudero-Adán, E. Martin and A. W. Kleij, *J. Am. Chem. Soc.*, 2013, **135**, 1228-1231; (g)Y. Xie, T. T. Wang, X. H. Liu, K. Zou and W. Q. Deng, *Nat. Commun.*, 2013, **4**, 1-7; (h)D. Adhikari, S. T. Nguyen and M. H. Baik, *Chem. Commun.*, 2014, **50**, 2676-2678; (i)P. Styring and S. Supasitmongkol, *Catal. Sci. Tech.*, 2014, **4**, 1622-1630; (j)C. J. Whiteoak, N. Kielland, V. Laserna, F. Castro-Gómez, E. Martin, E. C. Escudero-Adán, C. Bo and A. W. Kleij, *Chem. Eur. J.*, 2014, **20**, 2264-2275.
9. (a)H. Zhou, W. Z. Zhang, C. H. Liu, J. P. Qu and X. B. Lu, *J. Org. Chem.*, 2008, **73**, 8039-8044; (b)Y. Kayaki, M. Yamamoto and T. Ikariya, *Angew. Chem.*, 2009, **121**, 4258-4261; *Angew. Chem. Int. Ed.*, 2009, **121**, 4258-4261; (c)H. Zhou, Y. M. Wang, W. Z. Zhang, J. P. Qu and X. B. Lu, *Green Chem.*, 2011, **13**, 644-650.
10. (a)Q. W. Song, L. N. He, Q. W. Jin, H. Yasuda and T. Sakakura, *Green Chem.*, 2013, **15**, 110-115; (b)X. Meng, Y. Nie, J. Sun, W. G. Cheng, J. Q. Wang, H. He and S. Zhang, *Green Chem.*, 2014, **16**, 2771-2778.
11. (a)J. Meléndez, M. North and R. Pasquale, *Eur. J. Inorg. Chem.*, 2007, **2007**, 3323-3326; (b)M. North and R. Pasquale, *Angew. Chem.*, 2009, **48**, 2990-2992; *Angew. Chem. Int. Ed.*, 2009, **48**, 2946-2948; (c)W. Clegg, R. Harrington, M. North and R. Pasquale, *Chem. Eur. J.*, 2010, **16**, 6828-6843.
12. (a)C. X. Miao, J. Q. Wang, Y. Wu, Y. Du and L. N. He, *ChemSusChem*, 2008, **1**, 236-241; (b)T. Chang, L. L. Jin and H. W. Jing, *ChemCatChem*, 2009, **1**, 379-383; (c)J. Melendez, M. North and P. Villuendas, *Chem. Commun.*, 2009, **18**, 2577-2579; (d)J. Melendez, M. North, P. Villuendas and C. Young, *Dalton Trans.*, 2011, **40**, 3885-3902; (e)M. North, P. Villuendas and C. Young, *Tetrahedron Lett.*, 2012, **53**, 2736-2740; (f)D. W. Tian, B. Y. Liu, Q. Y. Gan, H. R. Li and D. J. Darensbourg, *ACS Catal.*, 2012, **2**, 2029-2035; (g)D. W. Tian, B. Y. Liu, L. Zhang, X. Y. Wang, W. Zhang, L. N. Han and D. W. Park, *J. Ind. Eng. Chem.*, 2012, **18**, 1332-1338; (h)C. Martin, C. J. Whiteoak, E. Martin, M. Martinez Belmonte, E. C. Escudero-Adan and A. W. Kleij, *Catal. Sci. Tech.*, 2014, **4**, 1615-1621.
13. (a)T. Ema, Y. Miyazaki, S. Koyama, Y. Yano and T. Sakai, *Chem. Commun.*, 2012, **48**, 4489-4491; (b)T. Ema, Y. Miyazaki, T. Taniguchi and J. Takada, *Green Chem.*, 2013, **15**, 2485-2492.
14. P. Ramidi, N. Gerasimchuk, Y. Gartia, C. M. Felton and A. Ghosh, *Dalton Trans.*, 2013, **42**, 13151-13160.
15. M. Adolph, T. A. Zevaco, C. Altesleben, O. Walter and E. Dinjus, *Dalton Trans.*, 2014, **43**, 3285-3296.
16. R. C. Luo, X. T. Zhou, S. Y. Chen, Y. Li, L. Zhou and H. B. Ji, *Green Chem.*, 2014, **16**, 1496-1506.
17. T. Chatterjee, M. Sarma and S. K. Das, *Tetrahedron Lett.*, 2010, **51**, 1985-1988.
18. W. Y. Wu, S. N. Chen and F. Y. Tsai, *Tetrahedron Lett.*, 2006, **47**, 9267-9270.
19. Z. Bu, G. Qin and S. Cao, *J. Mol. Catal. A: Chem.*, 2007, **277**, 35-39.
20. (a)M. Ramin, J. D. Grunwaldt and A. Baiker, *J. Catal.*, 2005, **234**, 256-267; (b)A. Decortes, M. Martinez Belmonte, J. Benet-Buchholz and A. W. Kleij, *Chem. Commun.*, 2010, **46**, 4580-4582; (c)H. Vignesh Babu and K. Muralidharan, *Dalton Trans.*, 2013, **42**, 1238-1248.
21. G. H. Eom, H. M. Park, M. Y. Hyun, S. P. Jang, C. Kim, J. H. Lee, S. J. Lee, S. J. Kim and Y. Kim, *Polyhedron*, 2011, **30**, 1555-1564.
22. G. Will, G. Boschloo, S. N. Rao and D. Fitzmaurice, *J. Phys. Chem. B*, 1999, **103**, 8067-8079.
23. J. H. Li, J. T. Wang, Z. W. Mao and L. N. Ji, *Inorg. Chem. Commun.*, 2008, **11**, 865-868.
24. R. C. Luo, R. Tan, Z. G. Peng, W. G. Zheng, Y. Kong and D. H. Yin, *J. Catal.*, 2012, **287**, 170-177.
25. C. Postmus, J. R. Ferraro and W. Wozniak, *Inorg. Chem.*, 1967, **6**, 2030-2032.
26. Y. J. Yadav, T. F. Mastropietro, E. I. Szerb, A. M. Talarico, S. Pirillo, D. Pucci, A. Crispini and M. Ghedini, *New J. Chem.*, 2013, **37**, 1486-1493.
27. (a)R. Tan, D. H. Yin, N. Y. Yu, Y. Ji, H. H. Zhao and D. L. Yin, *J. Catal.*, 2008, **255**, 287-295; (b)R. Tan, D. Yin, N. Yu, H. Zhao and D. Yin, *J. Catal.*, 2009, **263**, 284-291.
28. H. S. Kim, J. Y. Bae, J. S. Lee, O. S. Kwon, P. Jelliarko, S. D. Lee and S. H. Lee, *J. Catal.*, 2005, **232**, 80-84.
29. J. Sun, S. I. Fujita, F. Zhao and M. Arai, *Green Chem.*, 2004, **6**, 613-616.
30. (a)J. Sun, L. J. Han, W. G. Cheng, J. Q. Wang, X. P. Zhang and S. J. Zhang, *ChemSusChem*, 2011, **4**, 502-507; (b)J. L. He, T. B. Wu, Z. F. Zhang, K. L. Ding, B. Han, Y. Xie, T. Jiang and Z. Liu, *Chem. Eur. J.*, 2007, **13**, 6992-6997.
31. C. R. Qi, J. W. Ye, W. Zeng and H. F. Jiang, *Adv. Synth. Catal.*, 2010, **352**, 1925-1933.
32. J. M. Sun, S. I. Fujita and M. Arai, *J. Organomet. Chem.*, 2005, **690**, 3490-3497.
33. (a)S. S. Wu, X. W. Zhang, W. L. Dai, S. F. Yin, W. S. Li, Y. Q. Ren and C. T. Au, *Appl. Catal. A: Gen.*, 2008, **341**, 106-111; (b)J. Palgunadi, O. S. Kwon, H. Lee, J. Y. Bae, B. S. Ahn, N. Y. Min and H. S. Kim, *Catal. Today*, 2004, **98**, 511-514.
34. J. J. Peng and Y. Q. Deng, *New J. Chem.*, 2001, **25**, 639-641.
35. H. Y. Ju, J. Y. Ahn, M. D. Manju, K. H. Kim and D. W. Park, *Korean J. Chem. Eng.*, 2008, **25**, 471-473.
36. (a)S. Ghazali-Esfahani, H. Song, E. Păunescu, F. D. Bobbink, H. Liu, Z. Fei, G. Laurency, M. Bagherzadeh, N. Yana and P. J. Dyson, *Green Chem.*, 2013, **15**, 1584-1589; (b)F. Castro-Gomez, G. Salassa, A. W. Kleij and C. Bo, *Chem. Eur. J.*, 2013, **19**, 6289-6298.
37. W. L. E. Armarego and C. L. L. Chai, *Purification of Laboratory Chemicals, Fifth Edition*, 2003, Elsevier Science (USA), 2003.
38. D. J. Darensbourg, J. C. Yarbrough, C. Ortiz and C. C. Fang, *J. Am. Chem. Soc.*, 2003, **125**, 7586-7591.

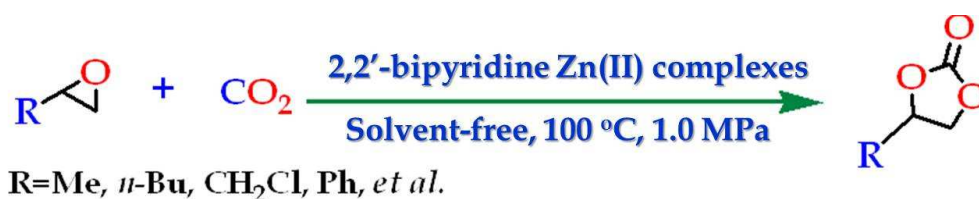
Graphical Abstract

Highly active bi-functional zinc catalysts based on robust and easy-to-handle *N*-chelating ligands for the synthesis of cyclic carbonates from epoxides and CO₂ under mild conditions

Rongchang Luo, Xiantai Zhou, Wuying Zhang, Zhongxiu Liang, Jun Jiang and

Hongbing Ji*

School of Chemistry and Chemical Engineering, Key Laboratory of Low-Carbon Chemistry & Energy Conservation of Guangdong Province, Sun Yat-Sen University, Guangzhou 510275, P.R. China



The zinc(II) complexes containing the rigid *N*-chelating ligand proved to be highly efficient and bi-functional catalysts towards the synthesis of cyclic carbonate from epoxide and CO₂ without the use of any co-catalysts or organic solvent.